Characterizing Morphometric and Nanomechanical Malignant Cell Features in a Rare Paediatric γδ T-acute Lymphoblastic Leukaemia: Insights from a Single Case Study Using Atomic Force Microscopy

Konstantin Bachvarov[1,†], Velichka Strijkova[2,3,†], Borislava Antonova[4,*], Maya Jordanova[1], Yoan Dimitrov[4], Svetla Todinova[3,*]

[1]*Department of Paediatric Haematology and Oncology,*
University Hospital "Queen Joanna"
8 Byalo More Str., Sofia, Bulgaria
E-mails: k.batschvarov@abv.bg, m.jordanova@sbaldohz.com

[2]*Institute of Optical Materials and Technologies "Acad. Jordan Malinowski"*
Bulgarian Academy of Sciences
Acad. Georgi Bonchev Str., Bl. 109, Sofia, Bulgaria
E-mail: vily@iomt.bas.bg

[3]*Institute of Biophysics and Biomedical Engineering*
Bulgarian Academy of Sciences
Acad. Georgi Bonchev Str., Bl. 21, Sofia, Bulgaria
E-mail: todinova@abv.bg

[4]*Medical Faculty, Medical University – Sofia*
2 Zdrave Str., Sofia, Bulgaria
E-mails: bantonova@medfac.mu-sofia.bg, yoandimitroff@gmail.com

[†]*The authors contributed equally to this work.*
[*]*Corresponding authors*

Received: May 29, 2023 **Accepted: August 14, 2023**

Published: December 31, 2023

Abstract: *The most common cancer in paediatric age is acute lymphoblastic leukaemia (ALL) which accounts for nearly a quarter of all cases of paediatric cancer. ALL cases are classified as B-cell or T-cell precursor ALL, based on their immunophenotypical features. Patients with T-cell ALL (T-ALL) comprise 10–15% of all newly diagnosed cases and are more prevalent in boys and in older age compared to the overall incidence peak age of ALL. In this case report, we present the morphometric and nanomechanical features of T-lymphoblasts derived from an 11-month-old infant with a rare subtype of γδ T-ALL with aggressive biological behavior. To investigate these features, we employed atomic force microscopy (AFM) and compared the blast cell deviations found in their nanostructure and elasticity to those of normal lymphocytes from a healthy child. The malignant T-lymphoblasts exhibited reduced roughness and Young's modulus values. This single case analysis demonstrates the potential of the AFM method to provide additional information regarding the characteristics of malignant cells and suggests its potential as a complementary approach for distinguishing neoplastic cells from normal cells. The application of AFM could potentially facilitate the introduction of in vitro tests to determine the efficacy of anti-leukemic treatments.*

Keywords: *Childhood T-cell acute lymphoblastic leukaemia, Atomic force microscopy, T-lymphoblast, Cell morphology, Membrane roughness, Young's modulus.*

Introduction

Leukaemia is the most common cancer in children [15]. It is generally categorized into acute and chronic. In acute leukaemia, immature hematopoietic cells of the myeloid or lymphoid

lineages, called myeloblasts and lymphoblasts, respectively, proliferate uncontrollably. The replacement of normal marrow by malignant cells subsequently results in a progressively increasing number of circulating immature blasts in the peripheral blood. Acute lymphoblastic leukaemia (ALL) is the most prevalent malignancy in childhood, accounting for approximately 25% to 30% of cancer cases in children under 15 years of age [22]. It can be categorized into B- or T-lymphoblastic leukaemia based on immunophenotypic characteristics, with approximately 85% of paediatric ALL cases being of B-cell lineage and the remaining 15% of T-cell lineage. Patients with T-cell ALL (T-ALL) are more commonly males and older than the mean peak incidence age for ALL. T-ALL often exhibits aggressive disease behavior, resistance to chemotherapy, and a higher and earlier relapse risk rate compared to B-cell ALL [8, 21]. Case reports for patients with T-ALL expressing the γδ T-cell receptor (TCR) have described a higher risk for poor outcomes [18]. ALL displays a heterogeneous nature, and the leukemic transformation is associated with a series of genetic alterations [4]. Accurate risk stratification of T-ALL is crucial for better therapy options, which has been greatly improved by combining the biological characterization of leukemic cells through various investigation methods such as immunophenotyping, cytogenetic analysis, and genetic profiling.

A significant advance in the chemotherapy of leukaemias has been made in recent decades which is reflected by a high 5-year overall survival rate [13]. Treatment of ALL is based on conventional methods, such as chemotherapy and radiotherapy. However, some complications related to conventional therapies may decrease their effectiveness. New treatment options for paediatric patients are targeted therapy, CAR-T-cell therapy, and immunotherapy, which are administered along with chemotherapy [13].

In recent years, AFM has become a promising method for investigating the morphology and quantifying the morphometric and mechanical properties of cells and tissues in various health and disease conditions. AFM enables the assessment of cellular shape, surface topography, and membrane roughness at micro- to nanometer scales, providing valuable insights into cell characteristics such as adhesion, motility, and intracellular interactions [10, 11]. Additionally, AFM allows for the measurement of cell deformability, which is a crucial indicator of cell function and development [1, 2, 19, 23, 24].

In this work, we present a case of an 11-month-old child with a rare form of γδ T-ALL. The AFM method was applied to assess the topological, morphometric, and nanomechanical features of the blast cells. These characteristics were compared to those of normal lymphocytes obtained from an 8-year-old healthy child. Our results reveal significant changes in the cell morphology and elasticity of the patient's blasts that distinguish them from those of the control.

Case presentation

History and clinical presentation

An 11-month-old boy with normal premorbid history presented with recent symptoms of decreased vitality, gradual abdominal enlargement, high fever, and skin rash. Laboratory tests conducted at another hospital revealed extreme hyperleukocytosis, severe anaemia, and thrombocytopenia. Consequently, the patient was referred to the Department of Paediatric Haematology and Oncology for further diagnostic clarification and treatment.

Upon admission, the patient was in a compensated general condition. He was afebrile, without any significant mucocutaneous changes, and showed no pathological findings upon physical examination of other organs and systems, except for a severely enlarged liver and spleen,

both of which are enlarged by 7 cm below the costal arch. Laboratory tests conducted upon admission and during the further diagnostic workup are summarized in Table 1.

Table 1. Laboratory values upon admission and results of diagnostic tests

Parameter	Reference range	Patient's indices
WBC count (G/l)	3.5-10.5	292,22
Percentage of peripheral blast cells/bone marrow	0	Morphological: 100% in PB and 80% in BM Immunophenotypically: 90% in PB and 70% in BM
Immunophenotypical characteristics of the lymphoblasts from peripheral and bone marrow materials		Aberrant T-cell phenotype: middle to low FSC/SSC, low positive for CD45 and surface sCD3, but intense positive for intracytoplasmic cCD3. Positive for γδTCR+, CD7, CD56+, CD5+, CD2+, CD99+ and dual positive for CD4 and CD8. Negative for CD34, CD117, HLA DR, CD45RA and CD1a, as well as for intracytoplasmic cTdT, cMPO, and cCD79a.
Cytogenetics/FISH		t(8;14)(q24;q11) with *c*-MYC rearrangement
PCR		not identified
Hb, (g/l)	118-140	45
Platelet count, (G/l)	140-440	39
TP, (g/l)	48-76	52
Albumin, (g/l)	35-50	33
LDH, (U/l)	200-540	1540
Cells in liquor, (CSF)	up to 14-15/μl	12
Applied chemotherapy protocol		ALL IC-BFM 09
Treatment effect/outcome after 1st therapy phase		Delayed and incomplete remission* (MRD level of 0.3%). Regression of organomegaly and clearance of liquor pleocytosis.
Actual status		Persistent MRD, despite treatment intensification

Legend: WBC – white blood cells count; PB – peripheral blood; Hb – hemoglobin; TP – total protein; LDH – lactate dehydrogenase; PCR – polymerase chain reaction; FISH – fluorescent *in situ* hybridization; MRD – minimal residual disease.

Peripheral WBC count exceeded more than 30 times the normal values, with an abundance of pathological lymphoblasts observed in the differential count. Blast cells with the same morphology and immune phenotype were identified in the bone marrow (BM) and cerebrospinal fluid (CSF). Blast cell morphology on a BM smear is presented in Fig. 1. Blue arrows show abnormal cells – the majority of lymphoblasts are small with uniform characteristics of the nuclei and cytoplasm. Some of the blasts are larger with a similar high nucleocytoplasmic ratio.

Flow cytometry (FCM) analysis of peripheral blood (Fig. 2), BM, and CSF samples, using an extended leukaemia antibody panel, confirmed the precise lineage diagnosis of γδ T-ALL.

Genetic alteration with t(8;14)(q24;q11) and *c*-MYC rearrangement was found, consistent with similar cases reported in the literature [14]. No other classical molecular genetic abnormalities of clinical significance were identified through PCR analysis. Consistent with a high tumour burden the value of lactate dehydrogenase (LDH) was high. Treatment was started under Therapeutic protocol ALL IC-BFM 09 – A Randomized Trial of the I-BFM-SG for the Management of Childhood non-B Acute Lymphoblastic Leukaemia [5]. First therapy phase also named "induction" combines 4 cytostatic drugs. According to the protocol the accepted definition of remission is: < 5% blasts in BM and < 0.01% blasts by FCM. In the documented case a delayed and incomplete attainment of remission was reported.

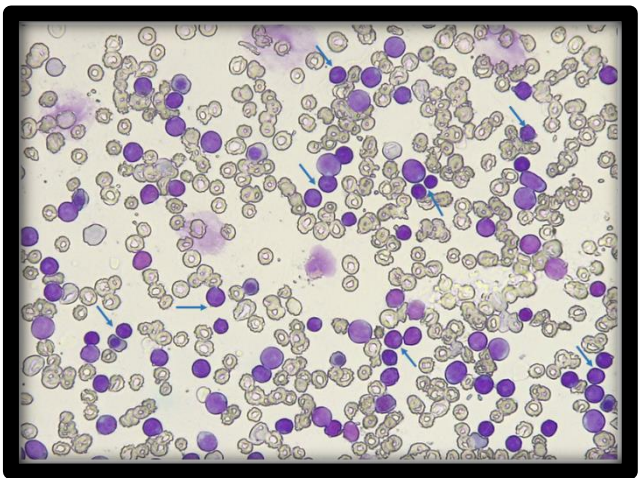

Fig. 1 Bone marrow smear at diagnosis (×40 magnification)

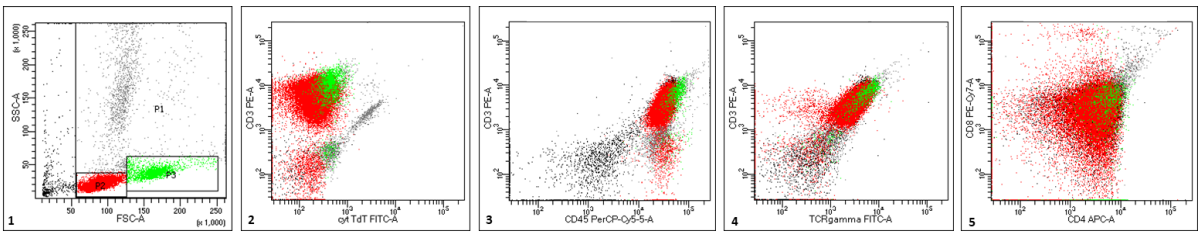

Fig. 2 FCM analysis of peripheral blood. Dot plots from the FCM analysis illustrating different size (FSC) and granularity (SSC) of 2 leukemic blast populations in the peripheral blood of the patient (red and green region on the 1st plot). Nevertheless, the intra cytoplasmatic and surface antigen phenotype confirmed their belonging to the same leukemic T-cell clone (cCD3+, sCD3+, γδTCR+, CD4/CD8 double+ presented in plots 2, 3, 4 and 5). Both blast groups may overlap with the 2 populations with different features identified by the AFM analysis (See Results – Population1 and 2).

Separation and storage of WBC for AFM measurements

All procedures were conducted in accordance with the ethical standards and approved by the Research Ethics Committee of Medical University – Sofia (protocol reference №10/25.05.22), following the guidelines of the 1964 Helsinki Declaration and its later amendments. Informed consent was obtained from the patient's parents as well as the parents of the control PB child donor.

WBC were isolated using gradient density mediums, specifically Ficoll-Paque PLUS (Global Life Sciences Solutions USA LLC, Marlborough, MA, USA), following the manufacturers' protocols. Venous blood was layered onto the medium and centrifuged, followed by a 2-step

washing procedure using phosphate-buffered saline (PBS). The separated white blood cells were then prepared for AFM analysis.

AFM investigation of T-lymphoblasts and normal lymphocytes

AFM measurements

An Atomic Force Microscope (MFP-3D, Asylum Research, Oxford Instruments, Santa Barbara, CA 93117, USA) was employed in contact mode to acquire topographic images of T-lymphoblasts derived from a patient with ALL and lymphocytes from a healthy donor (control). Quartz-like tips (Nanosensors, type qp-Bio) with a resonance frequency of 50 kHz, nominal spring constant of 0.3 N/m, and nominal tip radius of 8 nm (conical shape) were used for all AFM measurements. The main morphometric characteristics, incl. diameter, height, area, volume, and roughness value (R_{rms}), were determined using Gwyddion and IgorPro 6.37 software. Roughness analysis was performed in scanning areas of 2.0×2.0 μm² on the central part of the cells after the surface was preliminarily levelled to avoid the influence of the spherical profile. The R_{rms} value was calculated as the mean square root of the height distribution by the following equation:

$$R_{rms} = \sqrt{\sum_{i=1}^{N} \frac{(z_i - z_m)^2}{(N-1)}},$$

where N is the total number of data points, z_i represents the height of the i^{th} point, and z_m is the mean height.

The AFM method used for measuring the elastic properties of cells is based on cell indentation. Young's modulus (Ea) was determined by analyzing the force-distance curves applying the Hertz model generated by IgorPro 6.37 software embedded into the AFM system. Force mapping was conducted on a grid of 32×32 points within a scan area of 2×2 μm^2 at the center of the cell.

To assess the statistical differences in the main morphometric and nanomechanical characteristics between T-lymphoblasts from the patient with ALL and the healthy control cells, a Wilcoxon signed-rank test was performed. A $p < 0.05$ was considered statistically significant.

AFM data analysis

The AFM data analysis included the topological, morphometric, and nanomechanical characterization of T-lymphoblast cells compared to healthy donor lymphocytes. Representative AFM images of cells obtained from the patient and the control PB are shown in Fig. 3. The control lymphocytes were observed to be evenly spaced on the coverslip (Figs. 3A and 3B) and exhibited a spherical shape (Fig. 3C). In contrast, malignant T-lymphoblasts displayed distinct differences in both quantity and arrangement on the substrate. As shown in Figs. 3D and 3E, the blast cells were significantly more abundant than the control cells and tended to cluster in groups of three or four cells, unlike the control lymphocytes. The observed images in Figs. 3D and 3E are typical of multiple scans conducted on the patient's sample. While the profile of the lymphoblasts was also spherical, their size differed from that of the control cells (Fig. 3F).

Furthermore, a detailed investigation of the morphometric parameters of the cells under study was conducted. The control cells exhibited similar sizes, with an average diameter of 9 ± 0.9 μm and a height of 2.9 ± 0.3 μm. Their mean area and volume values were 65 ± 11 μm^2 and 232 ± 56 μm^3, respectively (Table 2). In order to determine the membrane

roughness, a detailed examination of a high-resolution on a small scan area (2.0×2.0 μm^2) was performed for both control and patient cells. Representative high-resolution images of the cell regions used to determine the roughness value are presented in Fig. 4. The plasma membrane of the "healthy" cells exhibited slight folding with a roughness value of 24 ± 2 nm (Fig. 4B, Table 2).

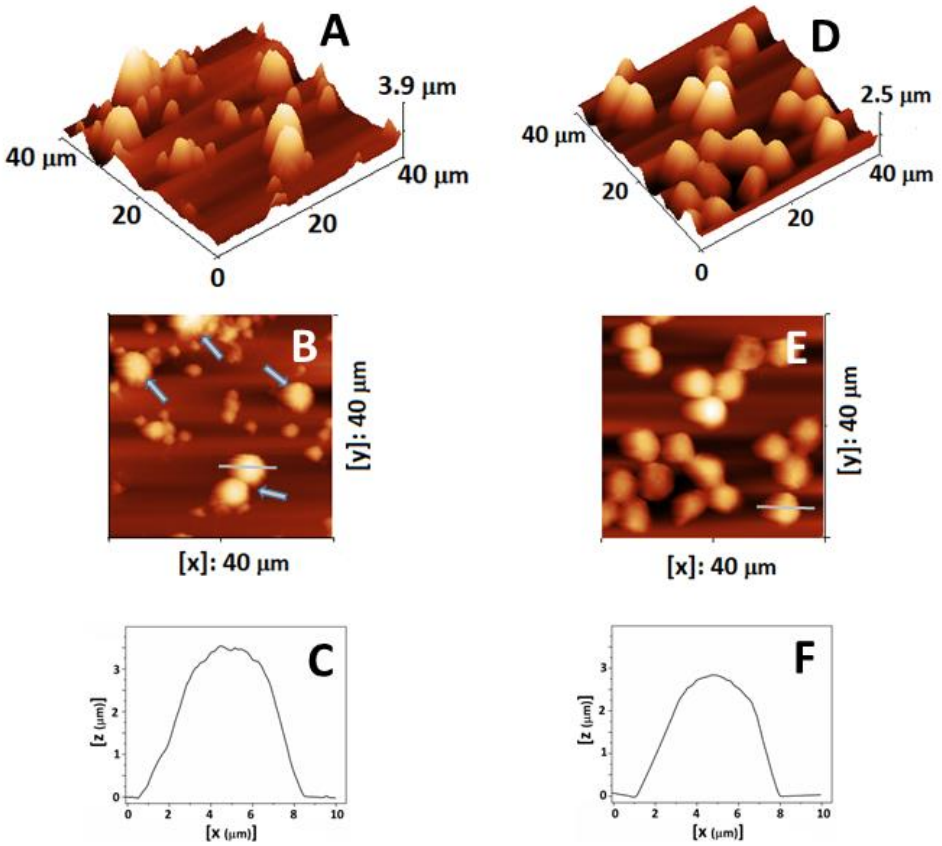

Fig. 3 Typical 3D and 2D AFM images of groups of normal lymphocytes from a healthy control donor (panel A and B with the arrows in panel B indicating the lymphocytes), and malignant T-lymphoblasts from the child with acute lymphoblastic leukaemia (ALL; panels C, and D) deposited on a glass coverslip. Adhered platelets, observed as small objects near the lymphocytes in panels A and B, and were also present in the sample. The cross-section plot profiles of the cells, defined by the grey line on the 2D topographical images of panels B and E, were presented in panels C and F, respectively. These images were captured using contact mode in air, at room temperature.

Table 2. Main morphometric and nanomechanical characteristics (average values ± SD)

Samples		Diameter, (μm)	Height, (μm)	Area, (μm^2)	Volume, (μm^3)	R_{rms}, (nm)	Ea, (MPa)
Control		9.3 ± 0.9	2.9 ± 0.3	66.5 ± 11	238.1 ± 56	24.1 ± 2.0	3.09 ± 0.7
ALL	Cell population1 (75%)	7.04 ± 0.3*	2.3 ± 0.2	39.0 ± 3.8*	184.3 ± 27*	17.8 ± 0.8*	0.87 ± 0.4*
	Cell population2 (25%)	9.8 ± 0.4	3.7 ± 0.3*	75.0 ± 5.8	489.5 ± 57*	15.1 ± 0.6*	2.18 ± 0.2*

*Indicates a statistically significant difference ($p < 0.05$) in the ALL values compared to the control

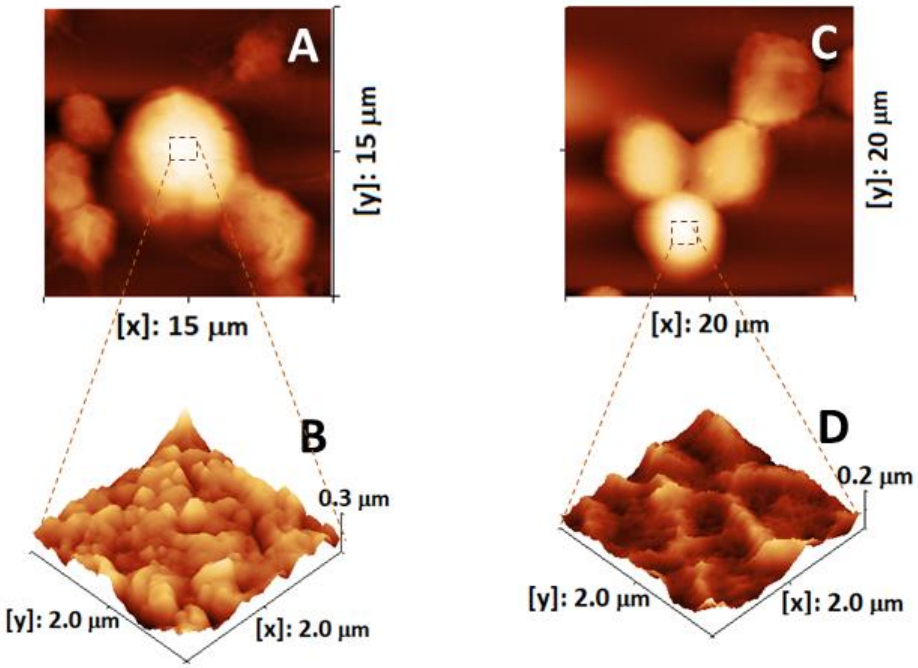

Fig. 4 Representative 2D images of single cells from the healthy donor (control, panel A) and T-lymphoblast cells from the patient (ALL, panel C). High-resolution images of the plasma membrane, indicated by a dotted square in the central part of the cell in Fig. A and C are presented in panels B and D, respectively.

The data analysis revealed the presence of two populations of T-lymphoblasts that differed from each other both and from the control cells. The larger one, referred to as Population1, showed lower values of diameter, spread area, and volume compared to the control cells (Table 2). The mean diameter and area of the Population2 patient's cells did not significantly differ from the control cells, while the height and volume showed higher values compared to the healthy lymphocytes. However, all these parameters were considerably higher than the corresponding values of Population1 lymphoblasts. The patient's cell membranes appeared relatively smoother compared to the controls (Fig. 4D). The roughness value R_{rms} was found to be lower for both patient populations' lymphoblasts compared to the healthy cells (Table 2).

Ea is an important parameter that reflects the mechanical properties of cell membranes. Fig. 5 represents the distribution of Ea values for all the leukemic and control lymphocytes. The average Ea value for the control cells was 3 ± 0.7 MPa with a wide range of values' distribution from 1.1 to 4.5 MPa.

The plot distribution of Young's modulus for T-leukemic cells exhibited a different pattern compared to that of healthy lymphocytes. The Population1 leukemic cells displayed a relatively normal distribution with a mean Ea value of 0.87 ± 0.4 MPa, which was 3 times lower than that of the control cells. The elasticity modulus of the cell membranes in Population2 was higher (2.18 ± 0.2 MPa) compared to Population1 but remaining lower than the control cells. Although the distribution analysis revealed some overlapping Ea values between Populaltion2 Ea and the lower Ea range of the controls, it is important to note that they were statistically distinguishable from each other.

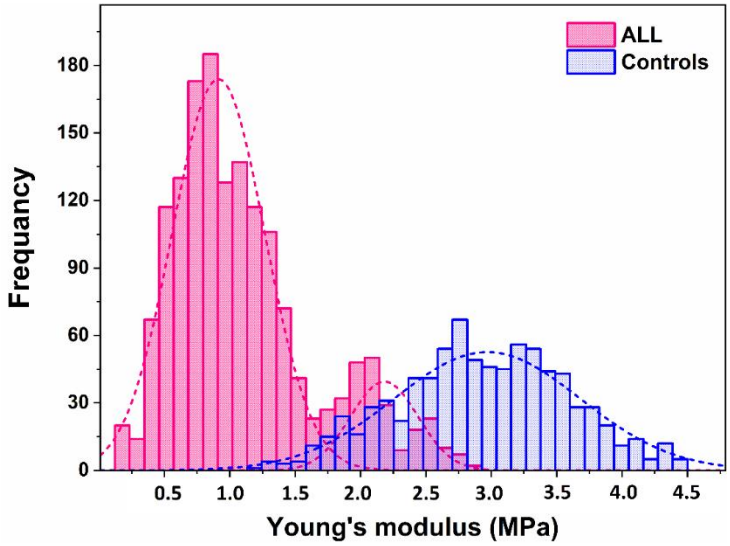

Fig. 5. Histogram of the Young's modulus distribution determined for T-lymphoblasts derived from a patient with acute lymphoblastic leukemia (ALL, red) and for control lymphocytes (Controls, light blue).

Discussion

In this single patient study, we made an important observation regarding the T-leukemic cells in our patient's sample. We identified two distinct types of T-lymphoblasts that differed in their morphometric characteristics and elastic properties. The majority of T-leukaemia cells (ca. 75%) exhibited smaller sizes and significantly reduced values of Young's modulus compared to normal leukocytes. According to the French-American-British (FAB) classification [3], which categorizes ALL into three subclasses (L1, L2, and L3), our case could be classified as L1 type, characterized by predominantly small blast cell size, although there were some variations in cell morphology on the bone marrow smears. A small portion (25%) of the patient lymphoblasts were found to have larger sizes (Fig. 2, 1st dot plot). It should be noted that the cells in this type of leukaemia are not entirely homogeneous.

The mechanical stiffness of cells plays an important role in tissue homeostasis, cell growth, division, and migration. The reduced stiffness of Population1 lymphoblasts suggests that these cells may have enhanced deformability, which could facilitate their migration through narrow capillary vessels and reduce their adhesion. This finding aligns with the observations of Michael et al. [19] upon mechanical properties of human leukaemia cells that may contribute to leukostasis. Similar to our findings, Skorkina et al. [20] demonstrated a decrease in lymphocyte stiffness in patients with chronic lymphocytic leukaemia, compared to normal lymphocytes. The lower stiffness of T-cells may explain their remarkable ability to transmigrate and move in dense tissues [6]. The altered mechanical properties of cells are associated with various disease conditions such as tumour formation and metastasis [7, 16].

A smaller proportion of blasts (ca. 25%) exhibited similar sizes to control cells but larger volumes. However, their stiffness was still lower than that of normal lymphocytes. The reasons behind these differences in the two lymphoblast populations remain unclear, and further studies are required to elucidate this particularity.

We also observed significant differences in the cell membrane structure between T-lymphoblasts and control lymphocytes. It should be noted that no significant difference was found in the R_{rms} value between the two populations of T-cells. We hypothesize that the higher

roughness value in healthy cells may be attributed to the presence of small projections of the plasma membrane, i.e., microvilli, which contribute to a more tightly folded surface. It has been established that membrane microvilli facilitate the binding and rolling of leukocytes on the vascular endothelium under flow conditions [17].

The reduced R_{rms} of the T-lymphoblasts may be a result of rearrangements in cytoskeletal proteins or a reduced amount or absence of microvilli. To support this hypothesis, further extensive studies employing additional methods need to be conducted.

It is worth noting that a similar abnormal lymphocyte structure, characterized by the absence of microvillus projections, has been observed in lymphocytes in Wiskott-Aldrich syndrome, which is associated with progressive deterioration of T-lymphocyte function [9]. Kim et al. [12] demonstrated that T-cell microvilli transmit signals to antigen-presenting cells, suggesting their involvement in T-cell activation. It is well known that blasts in acute leukemias are not immunocompetent cells. This accounts for the frequent and severe life-threatening infectious complications, characteristic of these diseases.

Conclusion

Our AFM measurements in a single case of a paediatric rare type of T-ALL revealed significant alterations in blast cell membrane nanostructure and elasticity compared to lymphocytes from a control peripheral blood sample. Moreover, the heterogeneity in size observed among T-blast cell populations indicated differences between them and the control cells.

This single case investigation provides additional insights into the mechanical properties of malignant T-lymphoblasts with potential implications in diagnostics and laboratory monitoring of therapeutic effects. The application of AFM shows potential in distinguishing neoplastic cells from normal lymphocytes. The application of AFM could facilitate the introduction of *in vitro* tests to determine the efficacy of anti-leukemic treatments.

Acknowledgments

Support of the Medical University – Sofia, Bulgaria, research project entry № 7430/19-11-21, contract № Д-140/14-06-2022, GRANT 22, to the Medical Sciences Council of Medical University – Sofia, is acknowledged. Research equipment of Distributed Research Infrastructure INFRAMAT, part of Bulgarian National Roadmap for Research Infrastructures, supported by Bulgarian Ministry of Education and Science was used in this investigation.

References

1. Alexandrova A., N. Antonova, M. Skorkina, et al. (2017). Evaluation of the Elastic Properties and Topography of Leukocytes' Surface in Patients with Type 2 Diabetes Mellitus Using Atomic Force Microscope, Series on Biomechanics, 31(3), 16-24.
2. Antonova N., A. Alexandrova, G. Melnikova, et al. (2019). Micromechanical Properties of Peripheral Blood Cells (Erythrocytes, Lymphocytes and Neutrophils) in Patients with Diabetes Mellitus Type 2, Examined with Atomic Force Microscope (AFM), Series on Biomechanics, 33(4), 3-11.
3. Bennett J. M., D. Catovsky, M. T. Daniel, et al. (1976). Proposals for the Classification of the Acute Leukaemias. French-American-British (FAB) Co-operative Group, British Journal of Haematology, 33(4), 451-458.
4. Bhojwani D., J. J. Yang, C. H. Pui (2015). Biology of Childhood Acute Lymphoblastic Leukemia, Pediatr Clin North Am, 62(1), 47-60.

5. Campbell M., L. Castillo, C. Riccheri, et al. (2009). Trial of the I-BFM-SG for the Management of Childhood Non-B Acute Lymphoblastic Leukemia, Final Version of Therapy Protocol from August 14 2009, https://www.bialaczka.org/wp-content/uploads/2016/10/ALLIC_BFM_2009.pdf
6. Friedl P., B. Weigelin (2008). Interstitial Leukocyte Migration and Immune Function, Nat. Immunol, 9, 960-969.
7. Guck J., S.Schinkinger, B. Lincoln, et al. (2005). Optical Deformability as an Inherent Cell Marker for Testing Malignant Transformation and Metastatic Competence, Biophysical Journal, 88(5), 3689-3698.
8. Karrman K., B. Johansson (2017). Pediatric T-cell Acute Lymphoblastic Leukemia, Genes Chromosomes Cancer, 56(2), 89-116.
9. Kenney D., L. Cairns, E. Remold-O'Donnell, et al. (1986). Morphological Abnormalities in the Lymphocytes of Patients with the Wiskott-Aldrich Syndrome, Blood, 68(6), 1329-1332.
10. Keren K. (2011). Cell Motility: The Integrating Role of the Plasma Membrane, Eur Biophys J, 40(9), 1013-27.
11. Khalili A. A., M. R. Ahmad (2015). A Review of Cell Adhesion Studies for Biomedical and Biological Applications, Int J Mol Sci, 16(8), 18149-18184.
12. Kim H. R., Y. Mun, K. S. Lee, et al. (2018). T Cell Microvilli Constitute Immunological Synaptosomes That Carry Messages to Antigen-presenting Cells, Nat Commun, 9(1), 3630.
13. Malczewska M., K. Kośmider, K. Bednarz, et al. (2022). Recent Advances in Treatment Options for Childhood Acute Lymphoblastic Leukemia, Cancers (Basel), 14(8), 2021.
14. Maziarz R. T., R. J. Arced, S. C. Bernstein, et al. (1992). A γδ+ T-Cell Leukemia Bearing a Novel t(8;14)(q24;q11) Translocation Demonstrates Spontaneous *in vitro* Natural Killer-like Activity, Blood, 79(6), 1523-1531.
15. Namayandeh S. M., Z. Khazaei, M. Lari Najafi, et al. (2020). GLOBAL Leukemia in Children 0-14 Statistics 2018, Incidence and Mortality and Human Development Index (HDI): GLOBOCAN Sources and Methods, Asian Pac J Cancer Prev, 21(5), 1487-1494.
16. Plodinec M., M. Loparic, C. A. Monnier, et al. (2012). The Nanomechanical Signature of Breast Cancer, Nature Nanotechnology, 7, 757-765.
17. Pospieszalska M. K., K. Ley (2009). Dynamics of Microvillus Extension and Tether Formation in Rolling Leukocytes, Cell Mol Bioeng, 2, 207-217.
18. Pui C. H., D. Pei, C. Cheng, et al. (2019). Treatment Response and Outcome of Children with T-cell Acute Lymphoblastic Leukemia Expressing the Gamma-delta T-cell Receptor, Oncoimmunology, 8(8), 1599637.
19. Rosenbluth M. J., W. A. Lam, D. A. Fletcher (2006). Force Microscopy of Nonadherent Cells: A Comparison of Leukemia Cell Deformability, Biophysical Journal, 90(8), 2994-3003.
20. Skorkina M. Y., M. Z. Fedorova, A. V. Muravyov, et al. (2012). The Use of Nanomechanic Sensor for Studies of Morphofunctional Properties of Lymphocytes from Healthy Donors and Patients with Chronic Lymphoblastic Leukemia, Bull Exp Biol Med, 154, 163-166.
21. Teachey D. T., C. H. Pui (2019). Comparative Features and Outcomes between Paediatric T-cell and B-cell Acute Lymphoblastic Leukaemia, Lancet Oncol, 20(3), e142-e154.
22. Ward E., C. De Santis, A. Robbins, et al. (2014). Childhood and Adolescent Cancer Statistics, 2014. CA Cancer J Clin, 64(2), 83-103.
23. Yu W., S. Sharma, E. Rao, et al. (2022). Cancer Cell Mechanobiology: A New Frontier for Cancer Research, Journal of the National Cancer Center, 2(1), 10-17.
24. Zemła J., J. Danilkiewicz, B. Orzechowska, et al. (2018), Atomic Force Microscopy as a Tool for Assessing the Cellular Elasticity and Adhesiveness to Identify Cancer Cells and Tissues, Seminars in Cell & Developmental Biology, 73, 115-124.

Konstantin Nikolov Bachvarov, M.Sc., MD
E-mail: k.batschvarov@abv.bg

Konstantin Bachvarov, MD, graduated from Medical University – Sofia, Bulgaria with a M.Sc. Degree in Medicine in 1995. He worked from 1996 to 1999 in CSMP – Sofia as a paediatrician and as an anaesthesiologist. Since 1999 he is working at the Department of Paediatric Haematology and Oncology, University Hospital "Queen Joanna", Sofia, Bulgaria. He has specialties in paediatrics and paediatric oncology/haematology.

Velichka Jordanova Strijkova, Ph.D.
E-mail: vily@iomt.bas.bg

Since 1999 Velichka Strijkova works at the Institute of Optical Materials and Technologies "Acad. Jordan Malinovski", Bulgarian Academy of Sciences (BAS) and since 2018 – at the Institute of Biophysics and Biomedical Engineering, BAS. She defended her Ph.D. Degree in Physical Chemistry, at the Institute of Optical Materials and Technologies "Acad. Jordan Malinowski" in 2014. In the last 6 years, her main activity has been related to the study of the surface and properties of various objects using an AFM – a full complement of operating modes for fluid and air operation, including contact/lateral force, non-contact AC mode, intermittent-contact (Q-control, phase, amplitude) mode, electric force microscopy, conductive c-AFM, force spectroscopy and force volume, I-V spectroscopy.

Head Assist. Prof. Borislava Antonova Mircheva, Ph.D.
E-mail: bantonova@medfac.mu-sofia.bg

Borislava Antonova is a Head Assistant Professor at the Department of Medical Physics and Biophysics, Faculty of Medicine, Medical University – Sofia. She is a graduate of the Faculty of Physics at Sofia University "St. Kliment Ohridski", M.Sc. Degree with major "Physics of Condensed Matter" in 1995. Assist. Prof. Mircheva received her Ph.D. Degree in Structure, Mechanical and Thermal Properties of Condensed Matter in 2009 at the Faculty of Physics, Sofia University "St. Kliment Ohridski". Her scientific interests are in the field of nanotechnology in medicine, thermodynamic methods for registration and analysis of changes in the state of plasma and liquor proteome in oncological and autoimmune diseases.

Assoc. Prof. Maya Nikolova Yordanova, Ph.D.
E-mails: m.jordanova@sbaldohz.com, mjordanova@medfac.mu-sofia.bg

Maya Yordanova is an Associate Professor in Paediatrics at the Medical University – Sofia, Bulgaria. She is a responsible physician for oncology and hematopoietic stem cell transplantation units at the Department of Pediatric Hematology and Oncology, University Hospital "Queen Joanna", Sofia, Bulgaria. Assoc. Prof. Yordanova received her Ph.D. Degree from Humboldt University, Berlin, Germany, in 2004. Her scientific work is in the field of flow cytometric analysis of normal and malignant cell populations.

Yoan Martinov Dimitrov, Student
E-mail: yoandimitroff@gmail.com

Yoan Dimitrov has completed his secondary education at the National Gymnasium of Natural Sciences and Mathematics "Acad. Lyubomir Chakalov" and is currently a student in the Medical Faculty of Medical University – Sofia, Bulgaria.

Prof. Svetla Zhelyazkova Todinova, Ph.D.
E-mail: todinova@abv.bg

Svetla Todinova graduated from Technical University – Sofia, with M.Sc. in Electronics. She received her Ph.D. Degree in Biophysics at the Institute of Biophysics and Biomedical Engineering, Bulgarian Academy of Sciences. Svetla Todinova is currently a Professor at the same institute. Her areas of interest include biomedical science, biomolecular interactions, microcalorimetry, electronics, circular dichroism, and atomic force microscopy.